

Anamorphic magnification using a chirped grating in grazing incidence mode

Tom Ditto^{*a} and Douglas A. Lyon^b

^aDeWitt Brothers Tool Co, POB 4000, Ancramdale, NY 12503

^bDept. of Computer Engineering, Fairfield University, Fairfield, CT

Abstract

We demonstrate that a grazing incidence configuration can be used with a surface relief diffraction grating having a shallow frequency chirp in one dimension and straight rules in the other to produce a long stand-off profilometer with significant anamorphic magnification.

1. Introduction

We have previously demonstrated range finding by diffraction with magnification features in chirped gratings using holographic optics¹ made by Leith-Upatnieks methods² in silver-halide depleted emulsions. Surface features of such gratings are characterized by chirped frequency spacing of rules. In profilometry applications both horizontal and vertical dimensions are affected by the grating. In the example of our prototype profilometer, “Moly”, the magnification feature is exploited to linearize the region of acquisition so that it is unaffected by perspective foreshortening.³ Moly has a rectangular acquisition window bounded by a 200 mm stripe profile vertical dimension with a 400 mm range reading at a 200 mm stand-off from the camera.

2. Chirped grating with straight rules in grazing incidence

In some applications where targets are tall relative to narrow bands of range, perspective foreshortening in profile dimension is a benefit. Gratings that have straight rules in one dimension and chirped rules in the other allow profile length to be seen at the same perspective afforded by the diffraction range finder lens and any associated structured illumination sheet of light. Our holographic gratings did not have straight rules, and we sought one that did.

A sample surface relief phase mask chirp grating with straight rules was obtained courtesy of Ibsen Micro Structures A/S.⁴ This sample grating (Figure 1) was originally intended for use as a master in the production of Bragg gratings in fiber optics. It is optimized for light at UV frequencies where the grating has high zero-order suppression. To achieve the suppression, it has a groove depth of approximately 220-250 nm (hence, it is inefficient in the red spectrum as will become evident in our experiment reported here). The Ibsen grating has a center period of 1067 nm with a linear chirp of 6.8 nm/cm over its length of 5 cm. It is 1 cm in height and sits on a 75 x 75 mm glass substrate. In the application for which it was made, the grating is illuminated by a collimated UV laser light source perpendicular to the grating plane, and the +/-first-order images constructively interfere within the fiber optic to form a Bragg grating inside a doped glass fiber.⁵ The 5:1 aspect ratio of the Ibsen grating is attributable to its use in the exposure of long and narrow fibers.

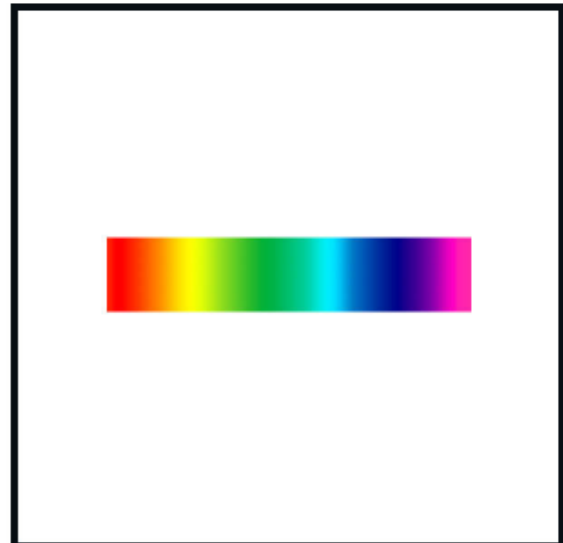


Figure 1 The Ibsen grating actual size. 75 mm x 75 mm substrate with internal 50 mm x 10 mm surface relief grating strip

* contact: scan3d@earthlink.net

As it happens, the long and narrow aspect ratio of the Ibsen phase mask grating also lends itself to a grazing incidence configuration for a diffraction range finder. Grazing incidence, as we use the term here, is exemplified by the Littman-Metcalf configuration used for tuning laser diodes.⁶ The Littman-Metcalf configuration is designated as a grazing incidence configuration, because a laser is injected at approximately 80 degrees to the grating plane normal. The cavity is used to lock a laser to resonant frequencies. This has nothing to do with diffraction range finding *per se*, but is recounted here as an example of grazing incidence with optical diffraction gratings. We have determined that a similar grazing incidence configuration will also work in a diffraction range finder where the detector collects light at an angle nearly parallel to the grating plane itself.

3. Geometric modeling with DiffCAD

We did not know whether a small grating element of 5 cm collects a coherent ray structure over a significant target distance of several meters. Littman-Metcalf cavities traverse a few millimeters and are not a predictor. We chose to geometrically model an experiment that utilized the length of our optical bench. Under this constraint of two meters length and 75 cm width, we used the DiffCAD program⁷ to model our grazing incidence diffraction range finder. The experimental conditions we selected were logged in the Java text window of DiffCAD as:

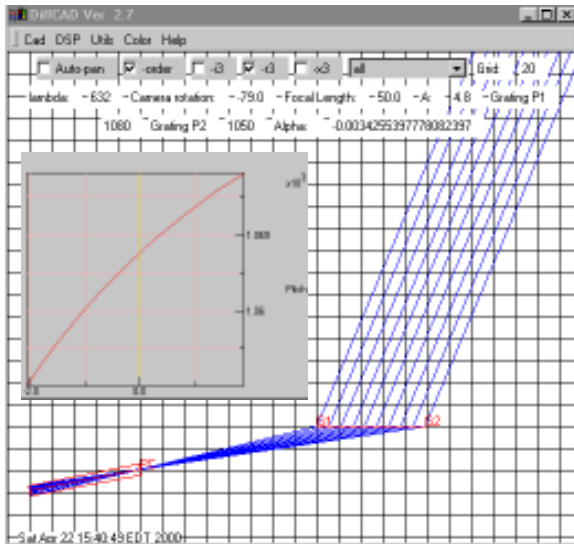


Figure 2 Camera model in DiffCAD showing Ibsen grating (G1-G2) and 50 mm lens (later replaced with 20 mm in actual experiment). Grazing angle is 11 degrees. Graph shows correspondence between pitch and focal plane position. Grid has 10 mm centers.

Figure 4 on the following page illustrates the experiment as a whole, but the scale of the drawing is such that details of camera and target regions require magnified views provided here by Figures 2 and 3. In fact, the stand-off of over a 1.5 meters is longer than any we have previously attempted with our diffraction range finding technique, notwithstanding that the geometric model predicts nearly the same sensitivity to range as a near-field stand-off of a few centimeters. DiffCAD is an extremely useful tool for designing diffraction range finders, but since it is based on the Grating Equation alone it does not provide coherence or efficiency predictions.

Laser rotation alpha = 0.00 degrees
 Laser co-ordinate x = 728.193 mm y = -45.572 mm
 Laser-grating plane crossing = -728.196 mm
 Camera rotation rho = -79.0 degrees
 Camera location x = -78.55 mm y = -19.16 mm
 Focal plane width A = 4.8 mm lens focal length F = 50.0 mm
 Camera to grating distance d = 19.1608 mm
 Laser terminus p1 = point = x = 728.31 mm y = 1985.24 mm
 Grating pitch P1 = 1080 nm P2 = 1050 nm
 Grating length L = 48.0 mm
 Laser wavelength Lambda = 632 nm

DiffCAD produced the predictions seen in Figures 2-4.

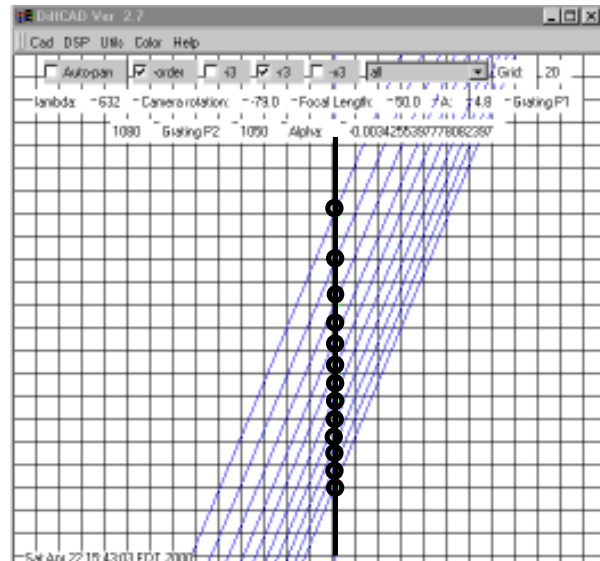


Figure 3 Target region as predicted by DiffCAD. Occlusion liability angle is about 23 degrees with a slight perspective foreshortening. Grid is on 1 cm centers and predicts about a 120 mm sensitivity.

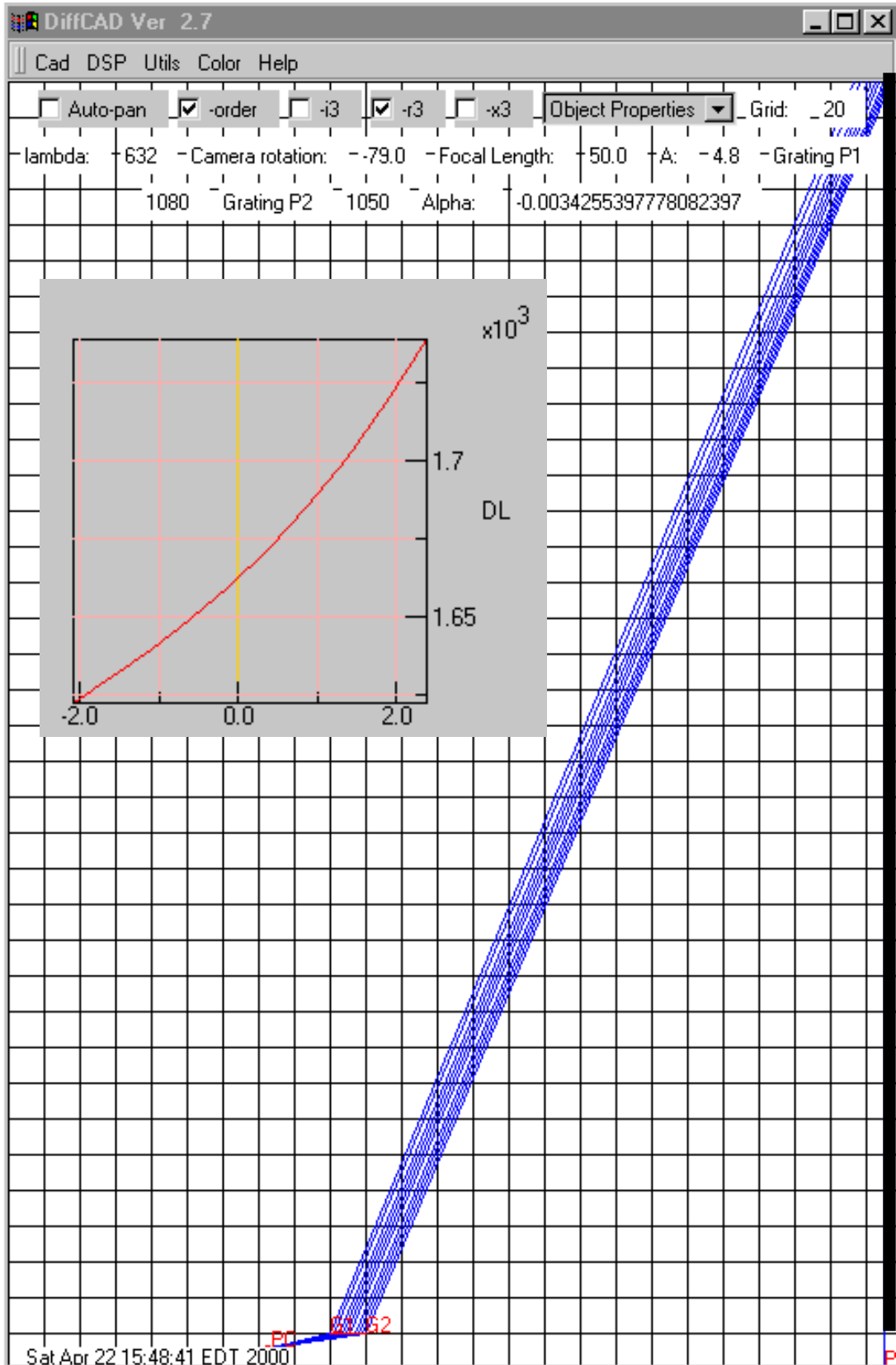


Figure 4 Overall view. Graph predicts range DL vs focal plane x in mm. Laser originates at P above and the target is on the upper right hand side of the graphic. This grid is on 5 cm centers.

4. Experiment

Geometric optics based on the Grating Equation do not adequately predict coherence over distance, and one could reasonably anticipate that real world behavior of this anamorphic telescope would be useless, the DiffCAD prediction notwithstanding. In fact, initial experimentation using a off-the-shelf 50 mm television camera lens showed considerable astigmatism. That experiment is not reproduced here. That 50 mm focal length lens was put aside for the special 4-20 mm “pinhole” zoom lens used in Moly⁸, and the camera in our DiffCAD model was changed from a third inch to a half inch CCD of high sensitivity. The resulting camera, lens and grating configuration used for the experiment can be seen in Figure 5. Micro positioners control rotation, translation and, in the case of the grating, tilt.

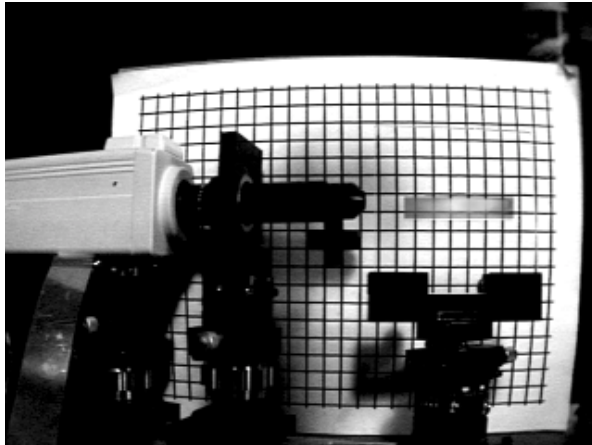


Figure 5 A high sensitivity half inch CCD with a nominal CS mount, the “pinhole” zoom lens and the Ibsen grating. The reference grid in the background has 1 cm spacings. Taken with a wide angle lens, hence the barrel distortion.

Alignment of the experimental system used a 45 degree incline and 90 degree vertical test block. We show in Figure 6 how these blocks appear in the zero-order by placing a first surface mirror in the place of the grating. These can be compared with their diffraction images in Figure 7. The vertical block in Figure 7 shows an unexpected bowing. The 45 degree block suggests a slight perspective foreshortening. The laser stripe was projected using a 10 degree Powell lens which did not fill the vertical dimensions of the field of view but provided over 1mW of energy per 7 mm length.

Those experienced in the art will immediately recognize from the right hand image in Figure 7 an anamorphic magnification feature that is not seen in conventional triangulation profilometry, a 1:1 reproduction of range data at a 23 degree occlusion liability angle. After our initial astigmatic results, we were also surprised that structured illumination line width was proportional to the dimensions of the sheet of light at the target. Ambient stripes in Figure 7 are artifacts of day light in the room. No band pass filter at the laser frequency was used.



Figure 6 Zero-order images of vertical and 45 degree test blocks created by using a mirror in place of the grating. The structured illumination spill below the test blocks illuminates a supporting pedestal and does not appear in the diffraction images of the same targets in Figure 7.

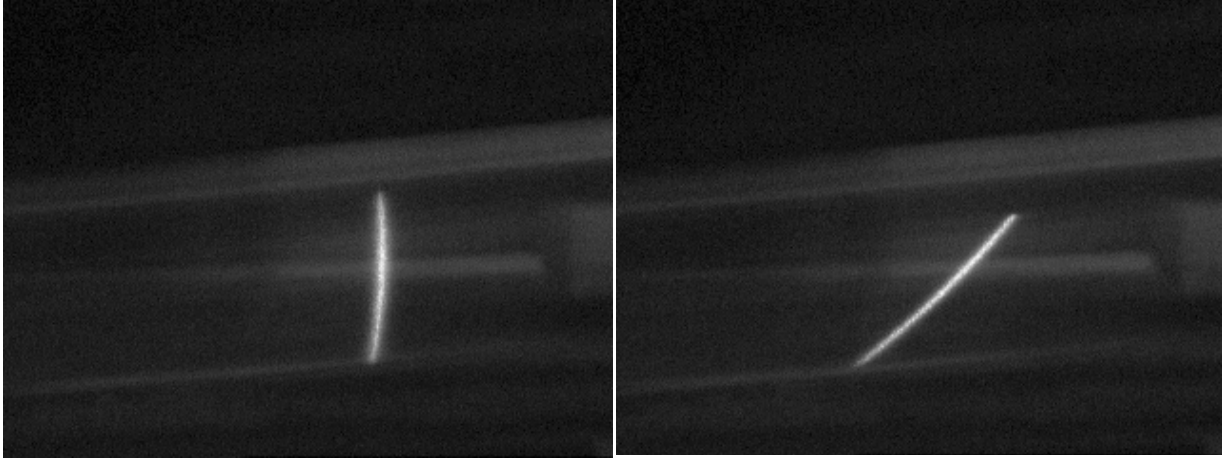


Figure 7 Diffraction image of vertical and 45 degree test blocks. The lefthand side image of a flat vertical surface exhibits bowing. The righthand image of a 45 degree incline is produced almost 1:1, height:distance.

We proceeded to place a mannequin as the target 3-D surface in the working region (Figure 8). Biff, as we call him, was the first acquisition target for our hand held scanner, Moly. The mannequin provides an intuitive grasp of the magnification feature and potential utility of this long stand-off profilometer. To obtain a profile across the vertical field-of-view, a 30 degree line generator based on a Powell lens⁹ was used, resulting in an average of 0.4 mW of energy per 7 mm length. The resulting images were near the noise floor of the camera. The Ibsen grating, made for service at UV frequencies, is inefficient at the 635 nm frequency used here.

The mind tells a viewer much about the range data in the zero-order image shown in Figure 8, but when the profile alone is shown as in Figure 9, the nose seems more like a cheek. Mathematically expanding the data would provide some suggestion of profile, but the optical magnification of the diffraction effect provides a much better dimensional portrait.

The diffraction effect is not a fixed anamorphic magnification but can be controlled as is illustrated in Figure 9 by showing a series of individual profiles that have been put together into a single image. The change in magnification is effected simply by rotating the grating plane relative to the camera. This also displaces the image to left and increases the occlusion liability angle. Autosynchronization of laser and grating is not as simple, since the laser position is 75 cm away from the camera in this setting, but there are both subtle and brute force means to introduce autosynchronization.¹⁰ There is also the suggestion that since magnifications go well above 1:1, the laser can be closer to the grating than in this initial experiment.

5. Applications and Conclusion

A decade ago a profilometer specification was posited to one of the authors by a Detroit sensor manufacturer for car door quality control. It would have a long stand-off to allow for intervening operators and machinery and enjoy a high “y to z” ratio, that is, use a wide structured illumination stripe but have a narrow range acquisition window. This experiment proves that such profilometers can be made with diffraction techniques. In manufacturing production lines, long stand-off to target is often a desired feature. The present experiment was conducted with a 2 inch length grating. *In situ* inspection of aircraft turbine blades would seem to be one application for the type of grating used in our experiment. If the grating length is increased then the stand-off to target is increased with unchanged resolution. Wing structure in aircraft manufacturing would seemingly benefit. The simplicity and low cost suggest autonomous vehicle navigation applications such as collision avoidance could be realized by attaching strips of embossed plastic grating to flat glass windows coupled with low cost cameras and low power IR lasers on either side of the vehicle. The idea that a narrow strip of material rather than an area collector suggests many configurations where space allocation and placement benefit, e.g. 3D surveillance. This inventor has not fully studied markets but has the expertise in competitive range finding technologies to confidently say that no equivalent range finder exists on the market today, because all prior anamorphic triangulation devices were limited to cylindrical refraction or reflection optics.

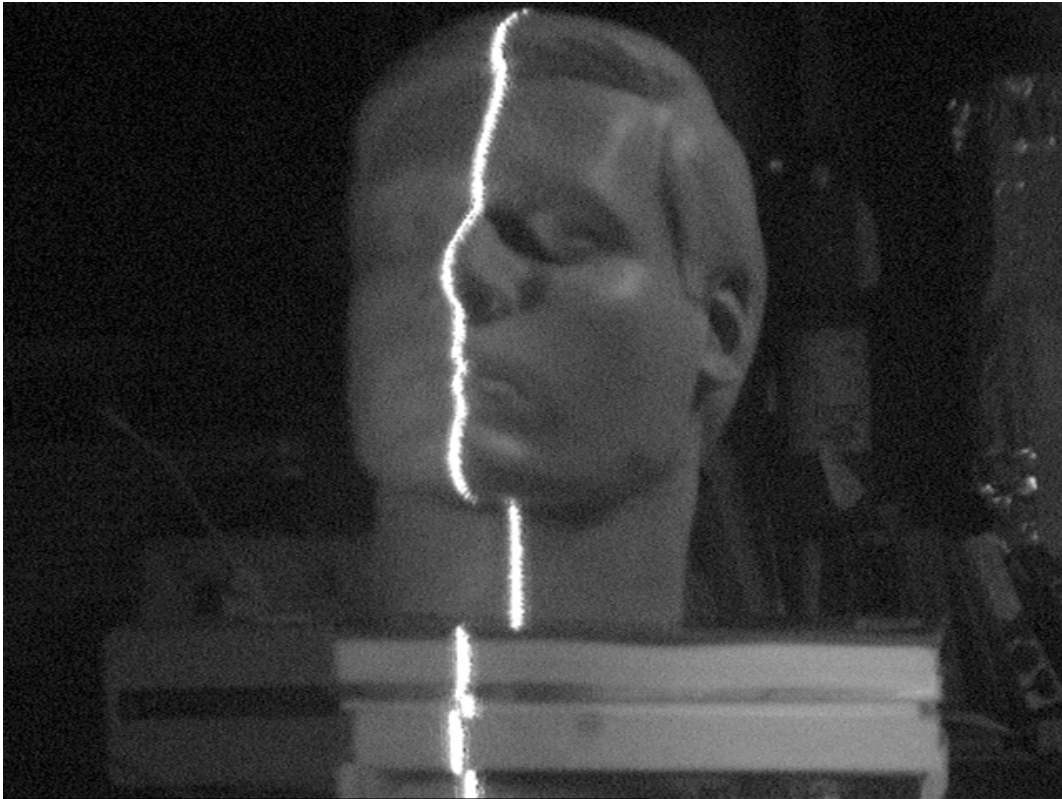


Figure 8 Zero-order image of Biff made using a mirror in place of the grating

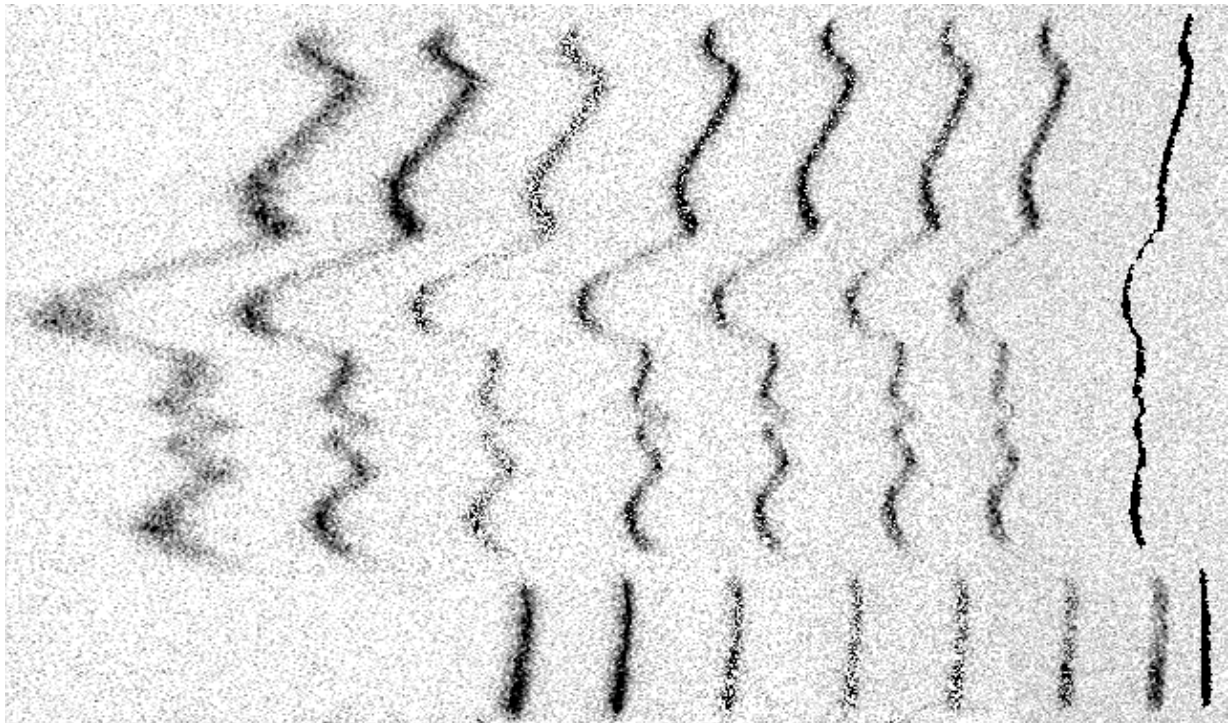


Figure 9 Various degrees of anamorphic magnification. The zero-order profile is on the extreme right hand side. The change in magnification is produced by simply rotating the grating. Background noise is the consequence of using a UV efficient grating in a red energy region, although laser lines do produce speckle.

We are using a grating that was intended for UV applications and has an inefficient groove relief for red light. One can reasonably expect that if surface relief geometries were tuned for a specific frequency, diffraction efficiencies of 80% are realizable in a grazing incidence configuration. The sample grating made by Ibsen could be remanufactured for red light. Since these are surface relief gratings, they hold the promise of low-cost replication in mass production settings. Furthermore, as far as sensitivity goes, the full-face of the grating is oriented toward the target assuring excellent gathering of incident flux thereby providing advantages in certain designs.

We have demonstrated that grazing incidence can be used in a surface relief diffraction grating with a chirp and straight rules to produce a long stand-off profilometer with a significant anamorphic magnification. Relative to refractive or reflective magnifiers, the grating method has excellent magnification with no apparent depth-of-field focus artifacts.

Acknowledgement

The authors wish to thank Kristian Buckwald of Ibsen Micro Structures A/S in Denmark for donating the phase mask grating used for this experiment.

References

- ¹ Tom Ditto, <http://home.earthlink.net/~scan3d/html/howdoesitwork.html>
- ² E.N. Leith and J. Upatnieks, "Reconstructed wavefronts and communication theory," *J. Opt. Soc. Am.* **52**, 1123-1130 (1962)
- ³ Tom Ditto and Douglas A. Lyon, "Moly: a prototype handheld three-dimensional digitizer with diffraction optics," *Opt. Eng.* **39**(1) 69-78 (January 2000)
- ⁴ <http://www.ibsen.dk>
- ⁵ Kenneth O. Hill et al, "Method of fabricating Bragg gratings using a silica glass phase mask and mask used by same", US Patent 5,367,588, November 22, 1994
also Pierre Sixt, "Phase Masks and Grey-Tone Masks," <http://www.fabtech.org/features/lithography/articles/body2.209.php3>
- ⁶ Francis S. Luecke, "Tuning System for External Cavity Diode Laser," US Patent 5,319,668, (June 7, 1994)
- ⁷ Douglas A. Lyon and Hayagriva V. Rao, *Java Digital Signal Processing*, originally published by MT Books, 1998, now available at <http://www.professor3d.com/book/book.htm>
- ⁸ These special lenses can be found listed at <http://www.mars-cam.com/frame/pinhole/v-zpl-xx.html>
- ⁹ Ian Powell, "Linear diverging lens", US Patent 4,826,299, May 2, 1989
- ¹⁰ M. Rioux, "Laser range finder based on synchronized scanners," *Appl. Opt.*, **23**, 3837-3844 (1984)